Holographic multi-focus 3D two-photon polymerization with real-time calculated holograms

Gaszton Vizsnyiczai,* Lóránd Kelemen, and Pál Ormos

Institute of Biophysics, Biological Research Centre, Hungarian Academy of Sciences, H-6726 Szeged, Temesvári krt. 62., Hungary

*gaszton@brc.hu

Abstract: Two-photon polymerization enables the fabrication of micron sized structures with submicron resolution. Spatial light modulators (SLM) have already been used to create multiple polymerizing foci in the photoresist by holographic beam shaping, thus enabling the parallel fabrication of multiple microstructures. Here we demonstrate the parallel two-photon polymerization of single 3D microstructures by multiple holographically translated foci. Multiple foci were created by phase holograms, which were calculated real-time on an NVIDIA CUDA GPU, and displayed on an electronically addressed SLM. A 3D demonstrational structure was designed that is built up from a nested set of dodecahedron frames of decreasing size. Each individual microstructure was fabricated with the parallel and coordinated motion of 5 holographic foci. The reproducibility and the high uniformity of features of the microstructures were verified by scanning electron microscopy.

OCIS codes: (230.6120) Spatial light modulators; (090.1760) Computer holography; (140.3300) Laser beam shaping; (050.6875) Three-dimensional fabrication; (230.4000) Microstructure fabrication.

References and links

1. S. Kawata, H. B. Sun, T. Tanaka, and K. Takada, "Finer features for functional microdevices - micromachines can be created with higher resolution using two-photon absorption," Nature **412**(6848), 697–698 (2001).
2. P. Galajda and P. Ormos, "Complex micromachines produced and driven by light," Appl. Phys. Lett. **78**, 249–151 (2001).
3. S. Maruo and H. Inoue, "Optically driven micropump produced by three-dimensional two-photon microfabrication," Appl. Phys. Lett. **89**, 144101 (2006).
4. M. Straub and M. Gu, "Near-infrared photonic crystals with higher-order bandgaps generated by two-photon photopolymerization," Opt. Lett. **27**, 1824–1826 (2002).
5. M. Deubel, G. von Freymann, M. Wegener, S. Pereira, K. Busch, and C. M. Soukoulis, "Direct laser writing of three-dimensional photonic crystal templates for telecommunications," Nat. Mater. **3**, 444–447 (2004).
6. Y. Liu, D. D. Nolte, and L. J. Pyrak-Nolte, "Large-format fabrication by two-photon polymerization in SU-8," Appl. Phys. A **100**(1), 181–191 (2010).
7. R. Di Leonardo, A. Búzás, L. Kelemen, G. Vizsnyiczai, L. Oroszi, and P. Ormos, "Hydrodynamic synchronization of light driven microrotors," Phys. Rev. Lett. **109**, 034104 (2012).
8. D. B. Phillips, S. H. Simpson, J. A. Grieve, R. Bowman, G. M. Gibson, M. J. Padgett, J. G. Rarity, S. Hanna, M. J. Miles, and D. M. Carberry, "Force sensing with a shaped dielectric micro-tool," Europhys. Lett. **99**, 58004 (2012).
9. L. Kelemen, S. Valkai, and P. Ormos, "Parallel photopolymerisation with complex light patterns generated by diffractive optical elements," Opt. Express **15**, 14488–14497 (2007).

#216573 - $15.00 USD Received 8 Jul 2014; accepted 3 Sep 2014; published 25 Sep 2014

10. J. Kato, N. Takeyasu, Y. Adachi, H.-B. Sun, and S. Kawata, "Multiple-spot parallel processing for laser micro-nanofabrication," Appl. Phys. Lett. **86**(4), 044102 (2005).
11. F. Formanek, N. Takeyasu, T. Tanaka, K. Chiyoda, A. Ishikawa, and S. Kawata, "Three-dimensional fabrication of metallic nanostructures over large areas by two-photon polymerization," Opt. Express **14**, 800–809 (2006).
12. L Kelemen, P. Ormos, and G. Vizsnyiczai, "Two-photon polymerization with optimized spatial light modulator," J. Eur. Opt. Soc. Rapid Publ.**6**, 11029 (2011).
13. S. Gittard, A. Nguyen, K. Obata, A. Koroleva, R. Narayan, and B. Chichkov, "Fabrication of microscale medical devices by two-photon polymerization with multiple foci via a spatial light modulator," Biomed. Opt. Express **2**, 3167–3178 (2011).
14. K. Obata, J. Koch, U. Hinze, and B. Chichkov, "Multi-focus two-photon polymerization technique based on individually controlled phase modulation," Opt. Express **18**, 17193–17200 (2010).
15. E. T. Ritschdorff, R. Nielson, and J. B. Shear, "Multi-focal multiphoton lithography," LAB ON A CHIP **12**(5), 867–871 (2012).
16. S. Bianchi and R. Di Leonardo, "Real-time optical micro-manipulation using optimized holograms generated on the GPU," Comput. Phys. Commun. **181**(8), 1444–1448 (2010).
17. N. Jenness, K. Wulff, M. Johannes, M. Padgett, D. Cole, and R. Clark, "Three-dimensional parallel holographic micropatterning using a spatial lightmodulator," Opt. Express **16**, 15942–15948 (2008).
18. http://www.nvidia.com/object/cuda_home_new.htm
19. R. Di Leonardo, F. Ianni, and G. Ruocco, "Computer generation of optimal holograms for optical trap arrays," Opt. Express **15**, 1913–1922 (2007).
20. A. Jesacher and M. Booth, "Parallel direct laser writing in three dimensions with spatially dependent aberration correction," Opt. Express **18**, 21090–21099 (2010).
21. http:freeglut.sourceforge.net
22. M. Persson, D. Engström, A. Frank, J. Backsten, J. Bengtsson, and M. Goksör, "Minimizing intensity fluctuations in dynamic holographic optical tweezers by restricted phase change," Opt. Express **18**, 11250–11263 (2010).

1. Introduction

Two-photon polymerization (TPP) is a widespread method to produce micron-sized structures with submicron resolution [1–8]. Complex 3D microstructures can be created such as photonic crystals [4, 5], microfluidic channels [6] or microstructures for holographic optical tweezers experiments [7, 8]. The method is based on the two-photon excitation of a negative photoresist by a femto-second laser with suitable wavelength. A high NA objective focuses the laser into a layer of photoresist, thus two-photon absorption is confined into a small, ellipsoid-like volume around the focus, called the voxel. 3D structures can be created by scanning the focus along a pre-defined trajectory inside the photoresist. Polymerization of a complex microstructure with fine features can take up to several minutes, therefore TPP microfabrication in large quantities can be a time consuming process.

A straightforward way to speed up the microfabrication process is to redirect the original laser beam into multiple polymerizing foci, allowing the better utilization of the available laser power, which is usually much higher, than required for a single focus. This can be achieved by various diffractive optical elements, such as kinoforms [9], microlens arrays [10, 11] and spatial light modulators (SLM) [12–15] modulating either the phase or the intensity of the laser beam. In the mentioned cases a 2D arrangement of foci is created, that is kept unchanged while the photoresist layer is translated in 3D during illumination, resulting in the creation of distinct identical microstructures by each focus. In this manner the fabrication time reduces proportionally with the number of applied foci. With phase modulating liquid crystal SLMs it is possible to create and dynamically rearrange multiple focal spots in 3D by holographic beam shaping. Such devices are the key elements of holographic optical tweezers, where they are used to create and move multiple optical traps in real-time [16]. This ability of an SLM has been used to demonstrate parallel single-photon polymerization of multiple identical microstructures by holographically created and translated focal spots [17]. However, TPP has not yet been presented in such a manner, as neither the parallel fabrication of a single three-dimensional structure with holographically translated multiple foci.

In this work we present two-photon polymerization of complex 3D microstructures, where

#216573 - $15.00 USD Received 8 Jul 2014; accepted 3 Sep 2014; published 25 Sep 2014

each individual microstructure was polymerized with the coordinated translation of multiple holographic foci. Such a fabrication was realized by continuously updating an electronically addressed SLM with new holograms, so that foci created by successive holograms exposed successive parts of the desired microstructure. Holograms were calculated real-time with the 60Hz refresh rate of the SLM on an NVIDIA CUDA graphics card by a self-developed C++/CUDA software. The recent development of CUDA technology enables to perform the hologram calculation by parallel computing on parallel throughput GPU architectures much faster than on CPUs. The software incorporates an OpenGL window to display the holograms on the SLM, as well as the control over a motorized microscope stage for repeated fabrication. To demonstrate the method, we designed a microstructure that is built up from a nested set of dodecahedron frames with decreasing size. As a dodecahedron frame has a 5-fold symmetry, this multi-dodecahedron structure was divided into 5 uniform segments and polymerized by 5 independent holographic foci.

2. Experimental setup

Figure 1 depicts the holographic two-photon polymerization system. The light source for two-photon polymerization is a femtosecond fiber laser (C-Fiber A 780, Menlo Systems, Germany) operating at 100 MHz frequency with 100 fs pulse length at 780 nm. The applied laser power was controlled with a half-wave plate ($\lambda/2$) in a rotational mount followed by a polarizing beam splitter cube (PBS). A pair of lenses (L_1, L_2) are used to expand the beam to match the SLM's (LC-R 2500, Holoeye Photonics AG, Germany) rectangular reflective surface along its shorter dimension. After reflection from the SLM the phase-shaped beam is imaged by a telescope lens pair (L_3, L_4) onto the back focal plane of a 100x 1.25 NA oil immersion objective (Zeiss Achroplan, Carl Zeiss, Germany) (OBJ) mounted on a Zeiss Axiovert 40 microscope. Propagation of the 0th and higher diffraction orders are blocked at the focus of lens L_3 by an aperture (A). The 1st order beams are focused into the photoresist layer sample (S) by the objective. Positioning and translation of the photopolymer sample are done by a motorized microscope stage (LS-2000, Märzhäuser Wetzlar GmbH & Co., Germany).

The test structures were made of SU-8 photoresist (Microchem, USA, resin type 2007) spin coated onto a 20 μm layer on a microscope cover slip. The layer was baked on a hot-plate prior to illumination for 2 and after it for 10 minutes at 100 C, and was developed by rinsing 3 times for 5 minutes in its developer (mr Dev-600) and finally in ethanol. Additionaly we used IPL photoresist (Nanoscribe GmbH, Germany) to visualize the polymerization process.

The holographic fabrication software, controlling the SLM and the microscope stage, runs on a desktop computer equipped with an NVIDIA Geforce GTX 560 Ti graphics card.

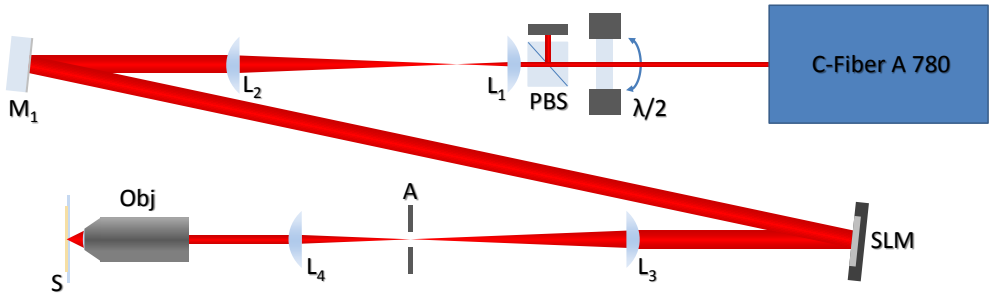

Fig. 1. Schematic layout of the holographic two-photon polymerization system.

#216573 - $15.00 USD Received 8 Jul 2014; accepted 3 Sep 2014; published 25 Sep 2014

3. Methods

3.1. Hologram calculation

An NVIDIA CUDA GPU was used to calculate holograms in real-time with the SLMs refresh rate. NVIDIA's CUDA [18] technology enables the development of applications that harness the computing power of the GPU, and can provide up to a few-hundreds of times speedup compared to CPU-utilizing applications. We have chosen to implement the weighted Gerchberg-Saxton (GSW) algorithm [19] due to its ability to calculate holograms for various numbers of foci with precise 3D arrangement and well controlled intensity. In the iterative procedure of the GSW algorithm a hologram ϕ is obtained as the phase of the weighted complex superposition of single focus holograms:

$$\phi_j = arg\left[\sum_m w_m e^{i\left(\Delta_j^m + \theta_m\right)}\right] \tag{1}$$

where ϕ_j is the jth pixel of the hologram, i is the imaginary unit, w_m and θ_m are the weight and phase of focus m, respectively, and Δ_j^m is the jth pixel of the hologram projecting focus m to coordinates (x_m, y_m, z_m) relative to the objective lens focal point:

$$\Delta_j^m = \frac{2\pi}{\lambda f}\left[x_j x_m + y_j y_m + z_m\sqrt{f^2 n_i^2 - \left(x_j^2 + y_j^2\right)}\right] \tag{2}$$

where x_j,y_j are the jth SLM pixel's coordinates on the back focal plane, f is the focal length of the objective lens and n_i is the refractive index of the immersion medium. In the iteration w_m and θ_m are initially set to 1's and to random numbers uniformly distributed in [0,2π], respectively, and are updated in each iteration step with respect to the complex field calculated on the positions of each focus:

$$V_m = \frac{1}{N}\sum_{j=1}^{N} e^{i\left(\phi_j - \Delta_j^m\right)} \tag{3}$$

$$w_m = w_m \frac{\langle |V_m| \rangle}{|V_m|} \tag{4}$$

$$\theta_m = arg\left(V_m\right) \tag{5}$$

where $\langle\rangle$ denotes averaging over all foci and N is the total number of pixels over V_m is calculated. As w_m are optimized during the iteration, deviations of $|V_m|$ from $\langle |V_m| \rangle$ are reduced, thus ϕ produces foci with highly uniform $I_m = |V_m|^2$ intensities. We note here that the term which z_m is multiplied with in Eq. (2) represents a spherical defocus wavefront that shifts the focal spot axially. This type of defocus wavefront is superior over the parabolic wavefront defined in [19] for high NA objectives designed to fulfill the sine condition [20]. To increase computational speed we calculated the hologram only on pixels that fall inside the objective's back aperture projection on the SLM.

Since the calculation time of GSW grows almost linearly with the number of foci and iterations, it is reasonable to express the calculation performance as *calculation time/number of foci/number of iterations* [16]. Our CUDA implementation of GSW achieves 0.165 ms/foci/iteration performance for holograms calculated over a circular area with 500 pixel radius. Since usually ~10 iterations are enough to produce holograms with high diffraction efficiency and uniformity, our software can calculate optimal holograms for up to 10 foci under the SLM's 16.666 ms refresh time. As an alternative for real-time calculation, the SLM can be refreshed by pre-calculated holograms stored on a hard drive. This method has obvious drawbacks in cases when a high number of holograms have to be displayed in a sequence, requiring large storage capacities.

#216573 - $15.00 USD Received 8 Jul 2014; accepted 3 Sep 2014; published 25 Sep 2014

3.2. *Holographic two-photon polymerization process*

The holographic two-photon polymerization process is controlled by a self-written C++/CUDA software incorporating the GPU hologram calculation procedure, an OpenGL window and control over the motorized microscope stage. The OpenGL window is created and managed with the FreeGLUT library [21], and serves to display the calculated holograms on the SLM. The calculated holograms were directly rendered from the GPU DRAM into an OpenGL texture through a Pixel Buffer Object, displaying the hologram on the SLM in less than 0.05 ms. Two separate text files are loaded upon startup of the software: one contains the voxel coordinates of the structure to fabricate and the other the microscope stage coordinates for repeated fabrication. Each row of the first text file holds coordinates of voxels to be exposed simultaneously. In the polymerization process a hologram for each row is calculated and displayed on the SLM sequentially, thus in every 16.666 ms each focus is re-created at an unexposed voxel position. A previously determined hologram that corrects for the SLM surface aberrations [12] is added to each hologram to achieve diffraction limited focus quality. For precise fabrication it is necessary to ensure that every hologram is displayed on the SLM for the same duration, so that every voxel is exposed uniformly. This can be achieved by enabling vertical synchronization for the OpenGL window, which ensures that the hologram in the OpenGL window is redrawn in synchrony with the SLM's refresh rate. As there is no mechanical movement involved in the process, the voxels of a microstructure can be exposed in arbitrary order.

4. Results

The plot of the designed multi-dodecahedron microstructure exposed by the foci of 5 holographic beams is shown on Fig. 2(a). The different colors depict the five complementary parts exposed simultaneously by the distinct foci.

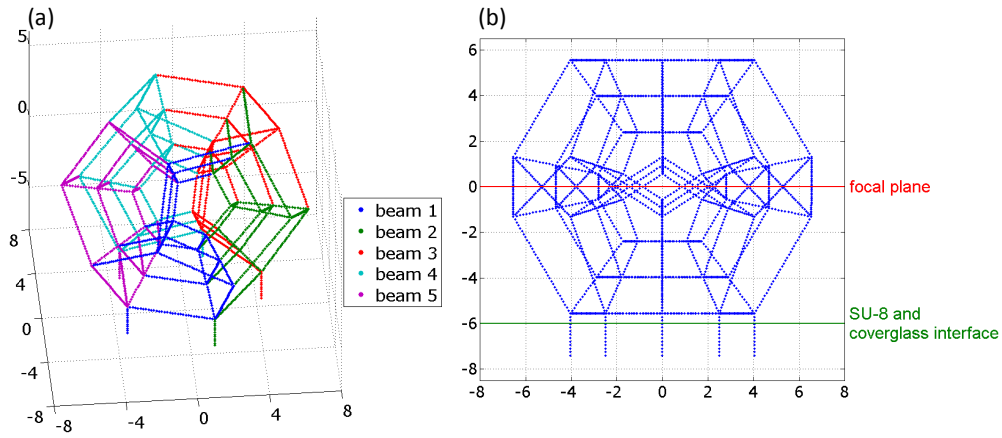

Fig. 2. (a) Three dimensional plot of the test microstructure voxel coordinates. Z-coordinates are relative to the focal plane of the objective. Different colors show voxels exposed by foci of different holographic beams. See Media 1 for the visualization of the scanning trajectories of the five foci. (b) Y-Z plot of the test microstructure revealing the relative positions of the focal plane and the coverglass-SU-8 interface. Axis units are in micrometers.

A 10 μm offset was added to both the x and y coordinates of the five holographic focal spots to separate the corresponding beams from the zero order, which therefore could be blocked at aperture A (Fig. 1). As diffraction efficiency for a holographic lens decreases with the absolute

#216573 - $15.00 USD Received 8 Jul 2014; accepted 3 Sep 2014; published 25 Sep 2014

z-coordinate of the holographic focus, it was reasonable to center the voxels z-coordinates in respect to the objectives focal plane. Consequently, the objectives focal plane was positioned ~6 μm over the glass substrates top surface that is inside the photoresist layer as illustrated in Fig. 2(b).

The microstructure was composed of 3 dodecahedron frames, with circumscribed sphere radii from 3 to 7 μm in 2 μm steps. With a uniform 150 nm voxel to voxel distance a total number of 2745 voxels needed to be exposed by 549 holograms each creating 5 foci. The holograms were calculated and displayed in real-time with the SLMs' 60 Hz refresh rate, which resulted in 9 μm/s scanning speed and 9.15 s fabrication time. We calculated every hologram with the same set of initial phases θ_m (Eq. (1)). This was necessary to minimize intensity fluctuations of the holographic foci that mainly arise from the random average phase change between consecutive holograms [22], especially when random θ_m is applied in the calculations.

The IPL photoresist was used to visualize the holographic two-photon polymerization process, since, in contrast to SU-8, it changes its refractive index immediately upon illumination. Figure 3 shows 6 representative frames from a video of an IPL microstructure polymerization recorded in our holographic TPP system.

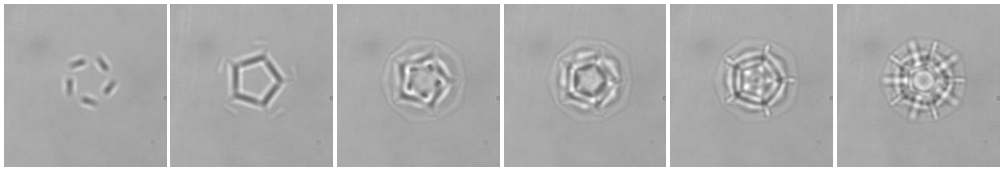

Fig. 3. Brightfield microscope images of the fabrication process visualized in IPL photoresist (Media 2).

Figure 4 shows scanning electron microscope images of holographically fabricated SU-8 test microstructures. The total applied laser power was 23 mW for the 5 holographic beams.

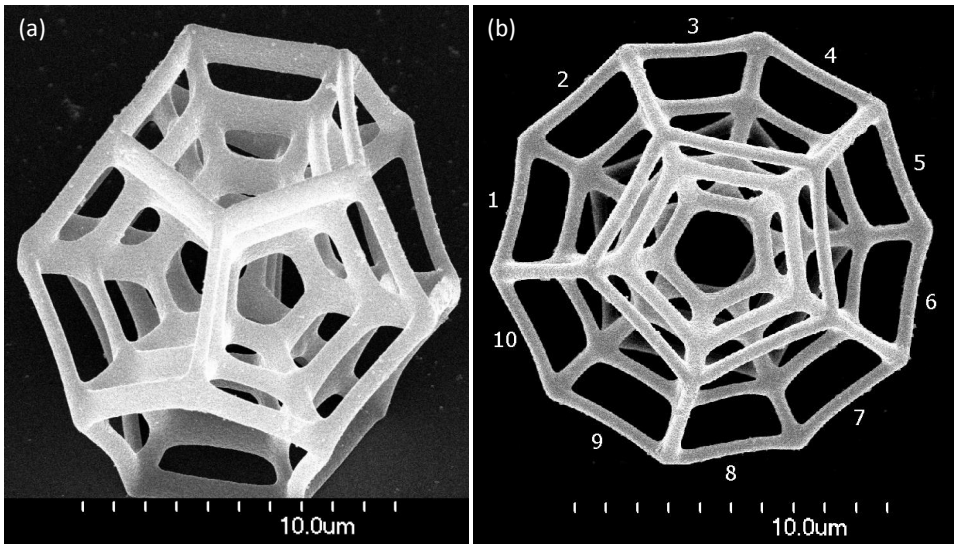

Fig. 4. Scanning electron microscope images of a holographically polymerized test structure, with viewing angle 45° (a) and top view (b).

#216573 - $15.00 USD Received 8 Jul 2014; accepted 3 Sep 2014; published 25 Sep 2014

As a merit of fabrication quality we measured the lateral thicknesses of the 10 outermost line segments of a microstructure (numbered on Fig. 4(b)). Each segments averaged thickness with its standard deviation is plotted on Fig. 5. The average of the ten thickness values is 454 nm with a standard deviation of 17.33 nm, which is 3.8% relative error. The thickness variation within the individual lines is also remarkably small: the average of standard deviations is 10.12 nm. These values indicate high uniformity among the five distinct focus intensities and also very low intensity fluctuation for each holographic focus during a holographic scan.

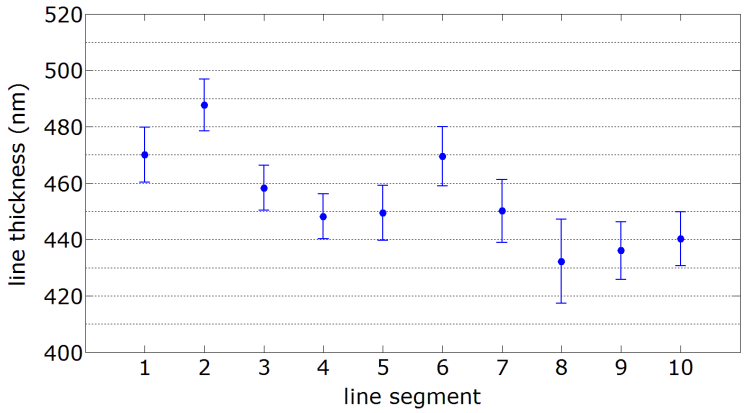

Fig. 5. The average and the standard deviation of thicknesses of the outermost line segments numbered on Fig. 3(b).

5. Conclusion

We demonstrated that complex 3D microstructures can be two-photon polymerized by multiple foci created and translated by a holographic spatial light modulator. Our implementation of the GSW algorithm can calculate optimized holograms for up to 10 foci under the SLMs refresh period on a CUDA GPU. This enabled us to efficiently generate five independent foci for the parallel holographic two-photon polymerization of multi-dodecahedron test microstructures. The uniformity of the foci and their temporal stability was verified by the very low thickness variation of the polymer lines of the test structure. The 9 μm/s scanning speed achieved with our 60 Hz refresh rate SLM can be further increased by the application of faster modulators: 200 Hz SLMs are already available and higher rate ones are expected to be released in the near future.

Acknowledgment

This research was supported by the EU and co-financed by the European Social Fund through the Social Renewal Operational Programme (TÁMOP-4.2.2.A-11/1/KONV-2012-0047 and TÁMOP-4.2.2.A-11/1/KONV-2012-0060) and by the Hungarian Science Research Fund (OTKA grant no. NN 102624). L. K. was supported by the Bolyai János Research Scholarship of the Hungarian Academy of Sciences.